POLITECNICO DI TORINO
Repository ISTITUZIONALE

Evaluating Injuries in Cyclist–Car Accidents using Conventional Dummies and Human Body Models

Original
Evaluating Injuries in Cyclist–Car Accidents using Conventional Dummies and Human Body Models / Tomassi, S., Scattina, A., Holder, D., Fehr, J.. - ELETTRONICO. - (2026). (International Research Council on Biomechanics of Injury Munich (DEU) 9 – 11 September 2026).

Availability:
This version is available at: 11583/3015876 since: 2026-09-24T11:28:20Z

Publisher:
International Research Council on Biomechanics of Injury

Published
DOI:

Terms of use:

This article is made available under terms and conditions as specified in the corresponding bibliographic description in the repository

Publisher copyright

(Article begins on next page)

01 October 2026

Evaluating Injuries in Cyclist–Car Accidents using Conventional Dummies and Human Body Models

Stefano Tomassi, Alessandro Scattina, Daniel Holder, Jörg Fehr

Abstract The study aimed to develop a workflow to simulate and analyse injury patterns in cyclist-to-car crash scenarios. The workflow is used to understand if initial analyses developed with conventional anthropometric test devices (ATDs) are enough to realistically assess injuries, or whether virtual simulations with human body models (HBMs) are required. Finite element models, combined with multi-body simulations, were implemented in MADYMO to study a lateral-frontal bicycle-car crash scenario. State-of-the-art ATD and HBM, both passive and active, were used to predict injury responses. To demonstrate broader applicability, the workflow was also used for early-stage safety-device evaluation. A simple deformable foam padding concept was introduced in virtual simulation and assessed for its ability to reduce tibial loading, illustrating the method's relevance for protective-system design. Virtual simulations showed that ATD and HBM have substantially different injury metrics and impact kinematics. Findings indicate that ATDs alone cannot capture key biomechanical behaviours relevant to common accident scenarios. Active HBMs enhance biofidelity, particularly in head and neck kinematics, and provide a more biofidelic basis for assessing injuries in vulnerable road users scenarios. The main insight of the research is that HBMs offer substantial benefits for evaluating cyclists' accident scenarios if compared with ATDs.

Keywords Active Human Body Model, Anthropometric Test Devices (ATDs), Cyclist, Finite Element Models, Positioning,

I. INTRODUCTION

In the European Union, cycling is the only means of transportation for which road fatalities have not decreased in recent years. Since 2010, approximately 2,000 cyclists per year have had fatal accidents on roads, contributing to almost 10% of all road fatalities in Europe [1]. Single bicycle crashes are the most frequent type of accident, but account on average only for the 17% of cyclists' fatalities [2]. Higher fatality rate occurs in cyclist to car crashes. Databases enriched through the years with real accident data show that the most common accidents between a cyclist and a car are bicycle side crashes [3-4]. In the type approval process of passenger vehicles, the protection of Vulnerable Road Users (VRUs), such as cyclists and pedestrians, is evaluated through impact tests using head and leg forms that strike the hood and bumper, respectively [5]. Despite the growing interest in evaluating the safety of cyclists, few studies attempt to assess injuries in cycling accident scenarios through physical tests, without a unified choice on the type of test performed [6-10]. Related works in VRU injury evaluation are based on virtual testing, specifically using finite elements methods (FEM) to reconstruct accidents stored in health databases or through experimental campaigns [11-13]. One proposed FEM tool is MADYMO, which has been widely used to evaluate the kinematics of bicycle accidents [6][14]. Despite MADYMO being still used by many car manufacturers, there are few recent works that use it for accidents analysis [15]. In virtual testing, Anthropometric Test Devices (ATDs) and Human Body Models (HBMs) are used to assess the injury criteria [13][16-18]. A sub-category of HBMs is composed of Active HBMs (AHBMs), in which muscular elements activate and impose a reaction force when a stimulus is provided [19]. Since a HBM realistically replicates the human body, it is expected to have different injuries values and impact kinematics for a specific injury scenario compared with an ATD [18][20]. Furthermore, AHBMs provide a more biofidelic response to impact if compared with passive HBMs [21-22]. Despite the comparison between ATDs and HBMs in occupants of passenger cars has been widely treated, at the best of author knowledge there is no work of this type in cyclists' accidents. Following part of what

S. Tomassi (e-mail: stefano.tomassi@polito.it) is a PhD student in mechanical engineering and Prof. A. Scattina is Professor of mechanical engineering at Politecnico di Torino, Italy. Dr D. Holder is a Group Leader at the Institute for Engineering Design and Industrial Design and Prof. J. Fehr is a Professor at the Institute of Engineering and Computational Mechanics, both at the University of Stuttgart, Germany.

[18] did for the analysis of injuries in a powered two-wheeler (PTW) crash scenario, the same workflow was applied here to a cyclist impact with a passenger car. The purpose of this work is to explore a methodology to achieve two research objectives.

1. Implement a virtual testing scenario to evaluate the performance of a safety device to reduce injury risks.
2. Evaluate differences in safety assessment outcomes when using ATDs and HBMs in cycling accidents.

The first research objective integrates safety-device performance evaluation into an early phase of product development [18]. The purpose of this approach is to emphasise the safety of VRUs in the vehicle development phase of transportation vehicles. The second objective research focuses on AHBMs to evaluate how muscular activation can influence the injury scores and the impact kinematics for an injury scenario. Previous work focused on differences between Passive HBMs (PHBMs) and AHBMs [20], while the focus of this work is to compare ATDs with HBMs in a cyclist accident. This paper presents quantitative differences in impact kinematics between the two models, quantitative differences in injury scores between the two models, and the effects of implementing a safety device.

II. METHODS

The components in the simulation environment were modelled using a combined Finite Element (FE) and Multi-Body (MB) strategy, following the methodology described in [6]. In particular, the car and the bicycle were modelled as kinematic chains of rigid bodies. This approach allowed computational efficiency, which was important given the focus of the study, that was the evaluation of injury scores and the comparison of ATDs and HBMs. Moreover, this simulation framework is intended to be used between the concept and the development stage described in [23] and briefly synthesised in Fig. 1.

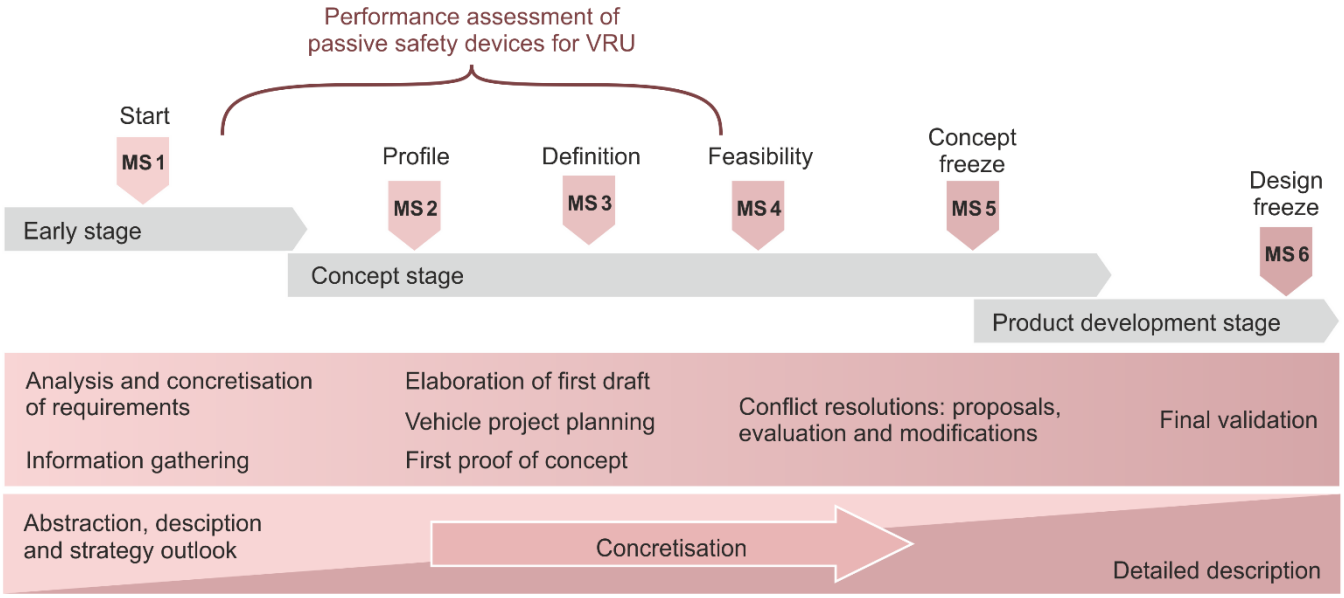

Fig. 1. Simplification of Reichelt [23] workflow and placement of the work in the product development process; between the early stage and concept stage, from Milestone (MS) 1 to Milestone 4.

The primary goal of the simulation was to understand whether a new safety device could introduce benefits in VRU protection and, if so, to what extent. For this reason, the main modelling efforts were focused on HBM and on the safety device. The simulation was developed in the MADYMO software environment, where proprietary ATDs and AHBMs are already included in the software library. As there is no standardized scenario for a bicycle crash, the motorcycle standard ISO13232-1 was selected, as it is the closest standardized scenario to the side bicycle crash, as described in [24] and depicted in Fig. 2.

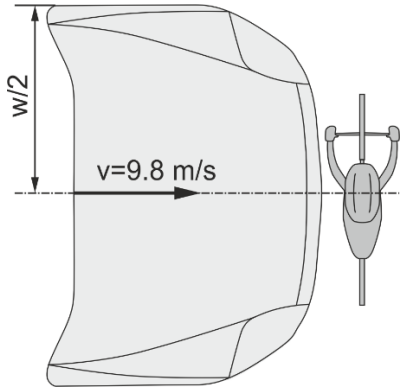

Fig. 2. ISO 132232:2005-1 scenario.

Passenger car and bicycle multi-body model

The passenger car used in this study is a Volkswagen Golf Series II model based on the models presented in [12] and depicted in Fig. 3. It has an overall mass of 1154 kg and the multi-body chain is composed of five bodies: the body of the car and four revolute joints that couple the four wheels with the body. The bicycle model has an overall mass of 28 kg and is composed of five rigid bodies connected through four revolute joints: the frame, the pedals, the two wheels and the handlebar. The mass and the inertial data of the bicycle are that of an E-bike proposed in [25]. A schematic of the multi-body chains of the bicycle is presented in Fig. 3.

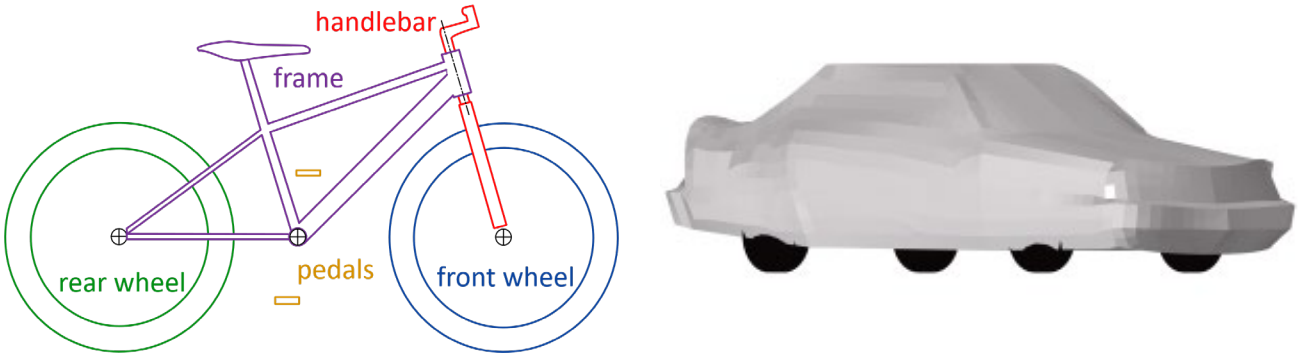

Fig. 3. Multi-body model of the bicycle and of the passenger car

Anthropometric Test Device and Active Human Body Model

The ATD used for this simulation was a Hybrid III 50th percentile male [26]. The reasons for using a Hybrid III instead of a Motorcyclist ATD (MATD) to represent a two-wheeler rider are the following:

1. The MATD is suited for integral helmets, rather than bicycle helmets [26].
2. Most of the physical tests used a Hybrid dummy (II or III) [7][9-10].
3. There is no MATD dummy available in LS-Dyna code at the best of author knowledge for future evaluations.
4. There is no variability in gender and percentile for a MATD [26].

The model included pre-defined load cell sensors to capture the required signals for injury criteria evaluation. The ATD was also modelled as a chain of rigid bodies, where the joints followed the physiological nature of the body joints. The HBM also represents a 50th percentile male (even though it has slightly different anthropometric data compared with the ATD) developed by MADYMO. Muscular activation was controlled by regulating an activation function for six muscle groups: neck, shoulder, spine, elbow, hip and knee. Each group contained the muscles elements that control the joint reference positions imposed by the user. The internal dynamics of the muscle replicate the physiological phenomena of muscular activation, including the reaction time and the neural delay. A schematic of the muscular control scheme is presented in Fig. 4, highlighting the input that the user must insert. The target signal represents the reference joint position over time, which the muscles track by activating

according to a PID control law that governs their dynamics. The initial activation is the percentage of maximum voluntary contraction (%MVC) that the muscles participating in the control of that degree-of-freedom have. For the sake of simplicity, it was set to 30% MVC for every muscle of the body, taking as reference [27]. This value does not replicate the actual %MVC of a cyclist, but during the crash phase a braced posture of the person is suggested to enhance more biofidelity [22]. The reaction time was set by default to 150 ms; it affects the muscular dynamics in response to an external perturbation that changes the joint position. The HBM was implemented in simulations both as AHBM and as PHBM: to set the HBM as passive, it is just needed to set the activation function to a null value for all the six groups.

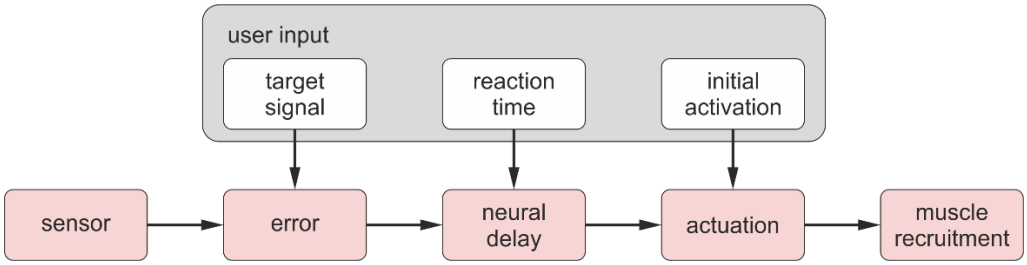

Fig. 4. Muscular activation scheme in MADYMO.

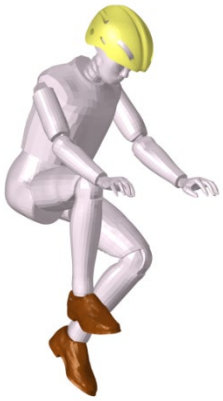

Fig. 5. ATD model.

TABLE I
MODEL DATA OF ATD AND HBM

ATD	Data	HBM
884	Sitting height (mm)	920
175	Standing height (cm)	176
78	Weight (kg)	75.3
43.6k	Elements	45.7k

Fig. 6. HBM model.

A comparison between the anthropometric data of the two models is shown in Table I, while Fig. 5 and Fig. 6 show the ATD and the HBM FE model implemented and positioned in the initial position of the simulations. Both models wear an urban type of helmet. The helmet was modelled with three parts: an exterior shell, discretized with shell elements, to contact with the vehicle, a core in polymeric foam whose function is to absorb the impact energy, discretized with 3D elements, and an interiors shell, modelled with shell elements, to contact with the head [28].To connect the helmet with the chin straps, seatbelt elements are used, and the chin strap is in contact with the chin [28]. The positioning of both ATD and HBM was performed through the MADYMO graphical user interface, which allows modifications of joint angles and visualise them in the pre-processing phase. In particular, the ATD and the PHBM were set immediately in the desired position on the bicycle. Once gravity is applied, the ATD and the PHBM entered in contact with the saddle through the pelvic area, the handlebar with the hands and the pedals with the feet. For the AHBM, the positioning has been performed by positioning in an initial desired state all the joints, applying muscular activation iteratively to the shoulder, knee and neck muscles joints. To make possible the action of the muscles force, the bicycle is fixed and the joints of the MB chain are constrained, otherwise the force would have moved the handlebar and the pedals. For the AHBM, the hands grip the handlebar to provide a better reaction force that stabilise the AHBM on the bicycle. Once the positioning phase and the crash happen, the contacts between the hands with the handlebar and the feet with the pedals are switched off. This is mainly intended because the fingers joints of the HBM are locked. If the contact was not disabled, the hands would have been stuck on the handlebar, leading to unproper kinematics of the HBM.

Impact-absorber model

The safety device used to reduce injury scores is an impact absorber made of polyurethane (PU) foam. The viscoelastic PU foam exhibits pronounced strain-rate dependent behaviour, remaining compliant under quasi-static loading while providing efficient energy dissipation and reduced peak forces under impact conditions. Its multi-impact capability and high specific energy absorption rate enable sustained protective performance without structural degradation, making it well-suited for repeated loading scenarios in injury biomechanics applications. A characterisation test of a PU foam for safety applications is described in [29]. The foam used in this work was the same as that used in [29]. The stress strain curves in strain rate dependency and quasi static condition are depicted in Fig. 9 and Fig.10. However, some limitations on the material modelling for this simulation should be considered and a final evaluation with FE simulation or real-world tests should be performed. Furthermore, the material modelling in [29] was defined for LS-DYNA solver, while model ran on MADYMO solver. For this reason, a larger amount of work would have been necessary to correlate with the physical drop-tower tests presented in [29]. Once the material had been tested in a virtual drop-tower test to check the energy-absorption performance, the specimen was enlarged in dimensions to cover a larger portion of the tibia. The specimen used for the drop test had dimensions of 80x80x20 mm. To cover a wider portion of the tibia, the dimensions were changed to 240x200x30 mm. Figure 7 shows the FE model of the virtual drop-tower test. Figure 8 shows the impact phase of the safety device with the leg. For this simulation, it was decided to place the padding foam in the region of first impact with the car, which in this case is the tibia. The reason for placing the protective device to the tibia is to reduce the effectiveness variability of the foam due to the different kinematics that might occur in ATD and HBMs.

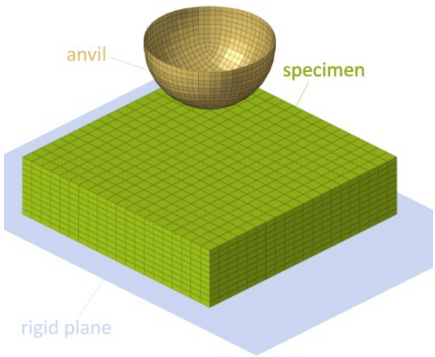

Fig. 7. FE model of the virtual drop test.

Fig. 8. Position of the foam during the impact phase.

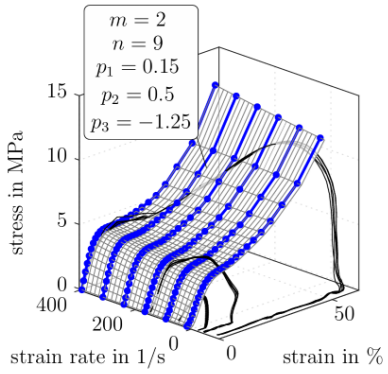

Fig. 9. strain rate dependent characterization of the PU foam.

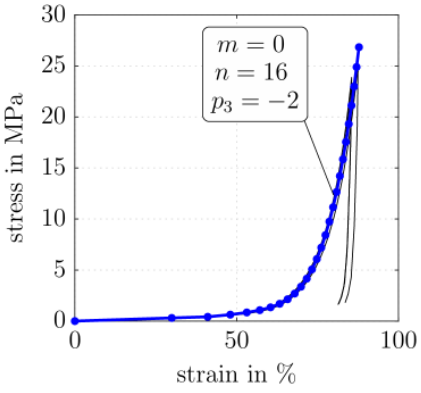

Fig. 10. Static stress-strain curve of the PU foam.

Injury criteria

Both the ATD and the HBM developed in Madymo have standard output keywords that allowed to collect relevant data to assess injury criteria. Injuries for ATD and HBM were quantitatively compared using the injury scores, which are listed by body region in Table II [30].

TABLE II
BIOMECHANICAL LIMITS FOR THE INJURY CRITERIA USED FOR COMPARISON

Body region	Criterion	Abbreviation	Limit
Head	Head Injury Criterion	HIC(36)	1000
	Resultant head acceleration	a_{3ms}	80 g over 3 ms
Neck	Neck tensile force	$F_{z,tens}$	3300 N
	Neck compression force	$F_{z,compr}$	4000 N
	Neck shear forces	F_{shear}	3100 N
	Neck rearward moment	$M_{y,rwd}$	57 Nm
	Neck forward moment	$M_{y,fwd}$	190 Nm
	Neck injury criterion	N_{ij}	1
Thorax	Resultant thorax acceleration	a_{max}	60 g
	Chest deflection	ThCC	75 mm
	Viscous Criterion	VC_{max}	1 m/s
Pelvis	Resultant pelvis acceleration	a_{max}	60 g
Femur	Femur axial force	$\|F_z\|_{max}$	10000 N
Tibia	Upper tibia index	UTI	1.3
	Lower tibia index	LTI	1.3

Computational resources

The simulations were performed on a workstation with an Intel Core i9-14900KF CPU, with a clock frequency of 6 GHz. The simulations were executed in shared-memory parallel processing (SMP), exploiting 12 of the 32 cores available for the CPU.

III. RESULTS

Six simulations are analysed in this section: ATD, PHBM, AHBM with and without foam. In this way, three research questions are investigated:

1. Which are the advantage of using a protective device in a cyclist accident.
2. Which are the difference in impact kinematics and injury assessments between an ATD and a HBM
3. How does the muscular activation changes impact kinematic and injury assessment in a HBM.

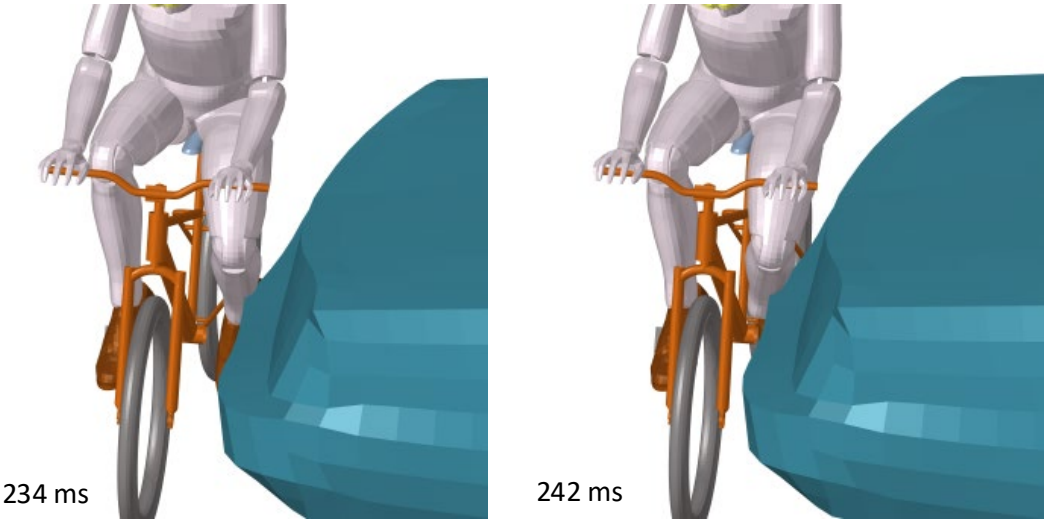

Fig. 11. Instants of impact of the tibia with the car (left) and with the bicycle (right).

ATD without safety device

The results obtained for the ATD-only simulation showed severe injuries in the head, neck and tibia regions, as can be seen in Table III. As can be seen from Fig. 11, the tibia was particularly loaded in the two impacts: the first one with the bumper of the car, and the second one with the frame of the bicycle. These impacts led to an impulsive peak of force exerted on the tibia.

When the head entered in contact with the hood, a spike of shear force and bending moment appeared. The frame on top view of the impact and the relevant plots are presented in Fig. 12. When the impact between the head and the hood occurred, as can be seen in Fig. 13, the alignment of the neck was such that the force exerted on the neck was mainly a shear force. A peak of shear force was visible for the ATD scenario at the impact instant between the head and the hood. The whole results of the different injury scores are presented in Table III. The injury indexes are defined as the ratio between the injury score and the limit for that injury criteria.

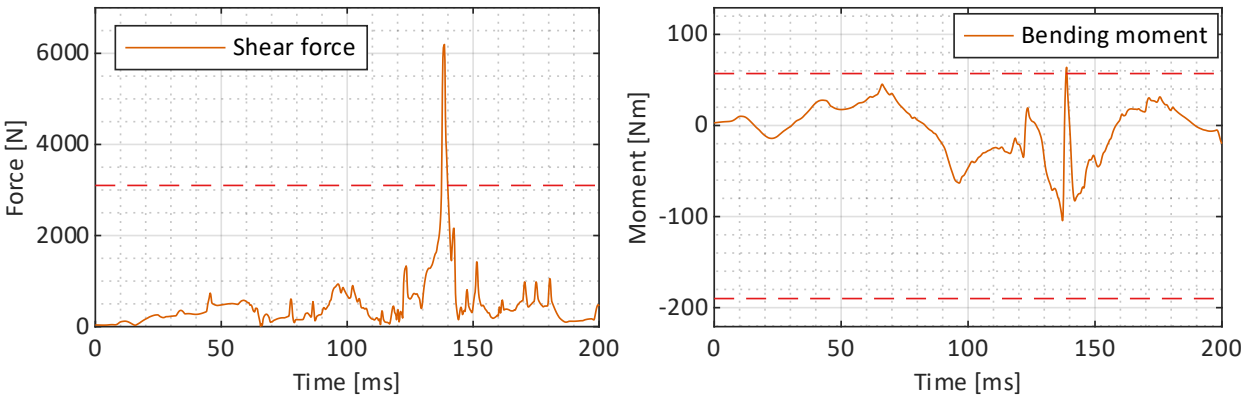

Fig. 12. Top view of head–hood impact instant and shear forces and bending moment of the neck.

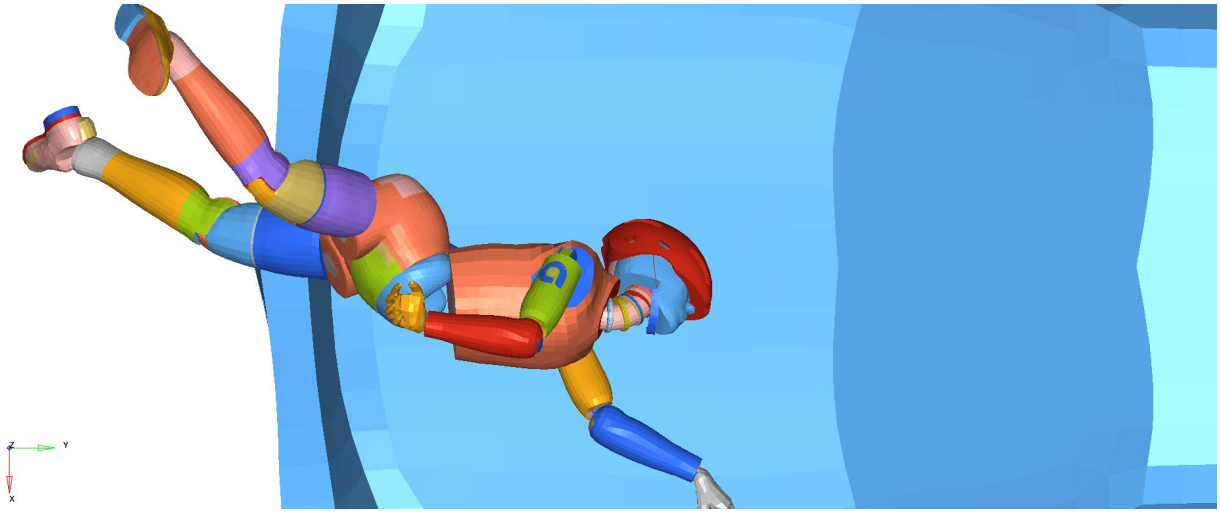

Fig. 13. Instant of the impact of the head with the hood (130 ms after the impact).

Introduction of impact absorber

The foam device was introduced with the primary purpose of reducing the peak force exerted on the tibia and reducing the loading rate by spreading the force over a wider range. As can be seen from Fig. 13, the loading rate and the peak force reduction were achieved by reducing the peak force and extending it over a longer time interval. The consequence is a reduction in the injury scores obtained for this scenario compared with the ATD without any safety device. As can be seen in Table III, the injury criteria related to the lower limb area (tibia and femur) were reduced, supporting the use of the safety device to decrease injury criteria.

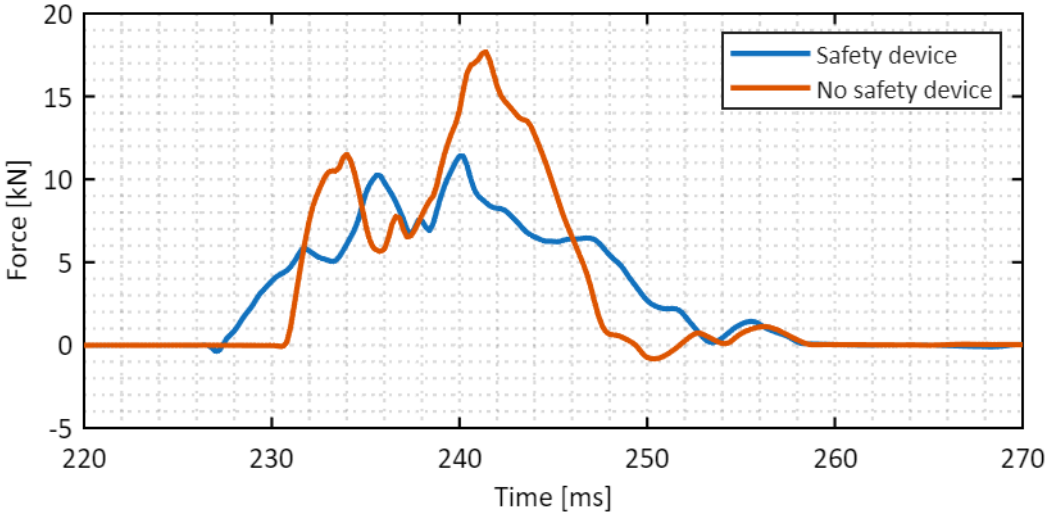

Fig. 14. Comparison between the force exerted on the tibia of the ATD with and without the safety device.

Impact kinematics and injury assessment

The use of the HBM showed changes in impact dynamics of the cyclist with the car. In Fig. 15, the trajectory of ATD, PHBM and AHBM heads are depicted quantitively. As can be seen, the head of the HBM covered a larger distance than that of the ATD because of the higher rebound in lateral bending. The main difference in impact kinematics between the AHBM and the PHBM was especially in the neck. The muscle activation of the AHBM provided less rotation of the neck in the vertical axis. At impact time, the AHBM was exposed to minor lateral whiplash effect if compared to the PHBM. The yaw angle time evolution, normalized with respect to the maximum yaw angle, is plotted in Fig. 16. In Fig. 17 the instant of time 200 ms after the impact is shown, where the difference in lateral rotation of the head is evident. The large values of head rotation in the PHBM simulation led the simulation to fail before the desired simulation time. In Fig. 18 the different kinematics of the ATD and the HBM during the crash are presented.

TABLE III

INJURY INDEX OBTAINED FOR THE DIFFERENT SIMULATIONS. THE VALUES OUTSIDE OF THE PARENTHESIS ARE THE INJURY INDEXES OBTAINED WITHOUT ANY PROTECTIVE DEVICE. THE VALUES INSIDE THE PARENTHESIS ARE THE INJURY INDEXES OBTAINED WITH THE PROTECTIVE DEVICE

Body region	Criterion	Injury index		
		ATD	PHBM	AHBM
Head	HIC(36)	4.64 (2.71)	3.74 (3.77)	2.55 (2.51)
	a_{3ms}	6.63 (1.77)	1.94 (2.49)	0.63 (0.65)
Neck	$F_{z,tens}$	0.85 (0.67)	0.65 (0.75)	0.33 (0.26)
	$F_{z,compr}$	0.02 (0.02)	0.01 (0.01)	0.03 (0.03)
	F_{shear}	1.95 (0.65)	0.29 (0.19)	0.34 (0.21)
	$M_{y,rwd}$	0.65 (0.71)	0.08 (0.08)	0.08 (0.06)
	$M_{y,fwd}$	1.10 (1.83)	0.13 (0.11)	0.50 (0.50)
	N_{ij}	1.68 (1.26)	0.47 (0.27)	0.16 (0.12)
Thorax	a_{max}	0.75 (1.00)	1.52 (1.32)	1.36 (1.10)
	ThCC	0.08 (0.06)	0.55 (0.50)	0.30 (0.27)
	VC_{max}	0.005 (0.003)	0.63 (0.62)	0.50 (0.54)
Pelvis	a_{max}	0.78 (0.63)	0.91 (0.86)	0.96 (1.03)
Femur	$\|F_z\|_{max}$	0.48 (0.32)	0.79 (0.82)	0.60 (0.69)
Tibia	UTI	6.10 (4.59)	0.99 (1.02)	1.16 (1.10)
	LTI	7.56 (9.1)	2.28 (2.16)	1.32 (1.22)

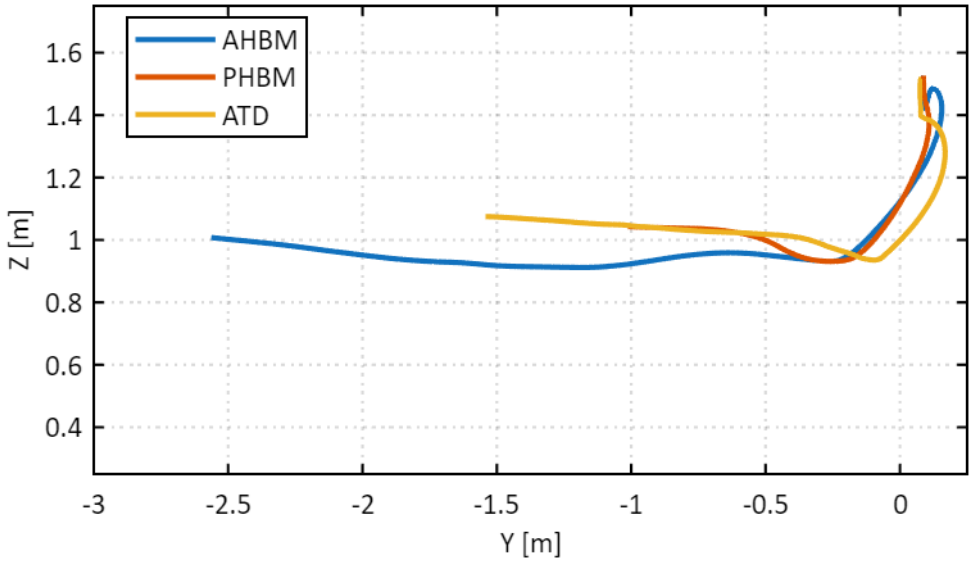

Fig. 15. Head trajectories for the three models during the crash phase

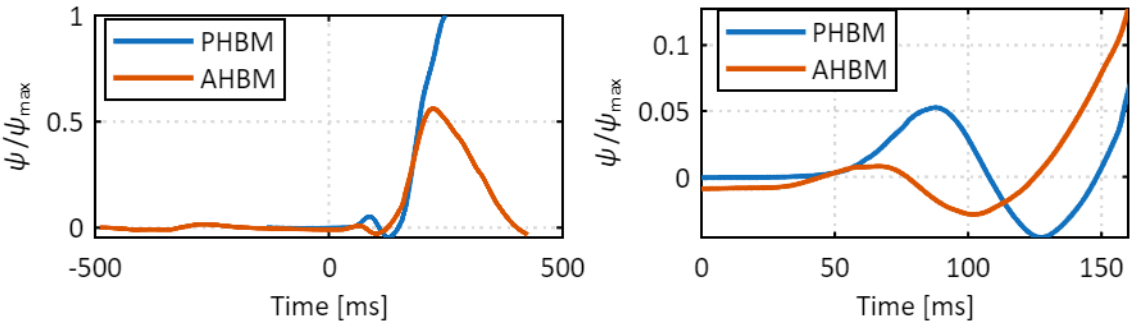

Fig. 16. Time evolution of normalized yaw angle of the head along whole simulation time (left) and after the impact phase (right).

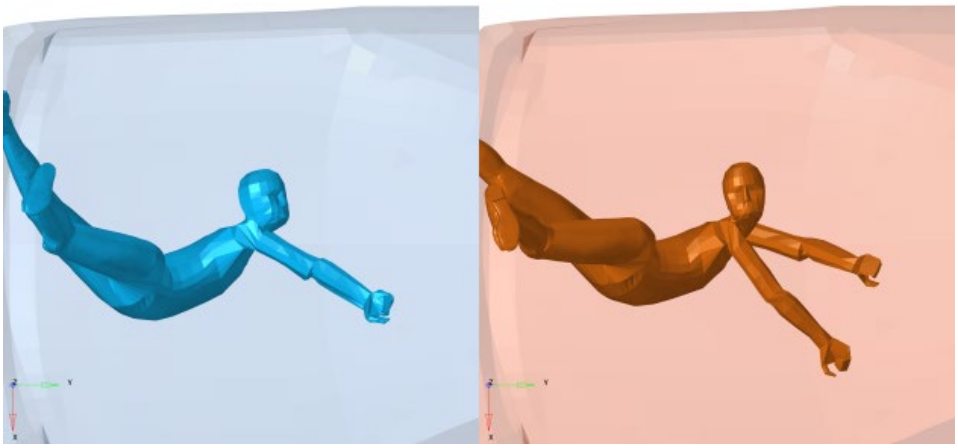

Fig. 17. Top view of AHBM (left) and PHBM (right) head rotation 200 ms after the impact.

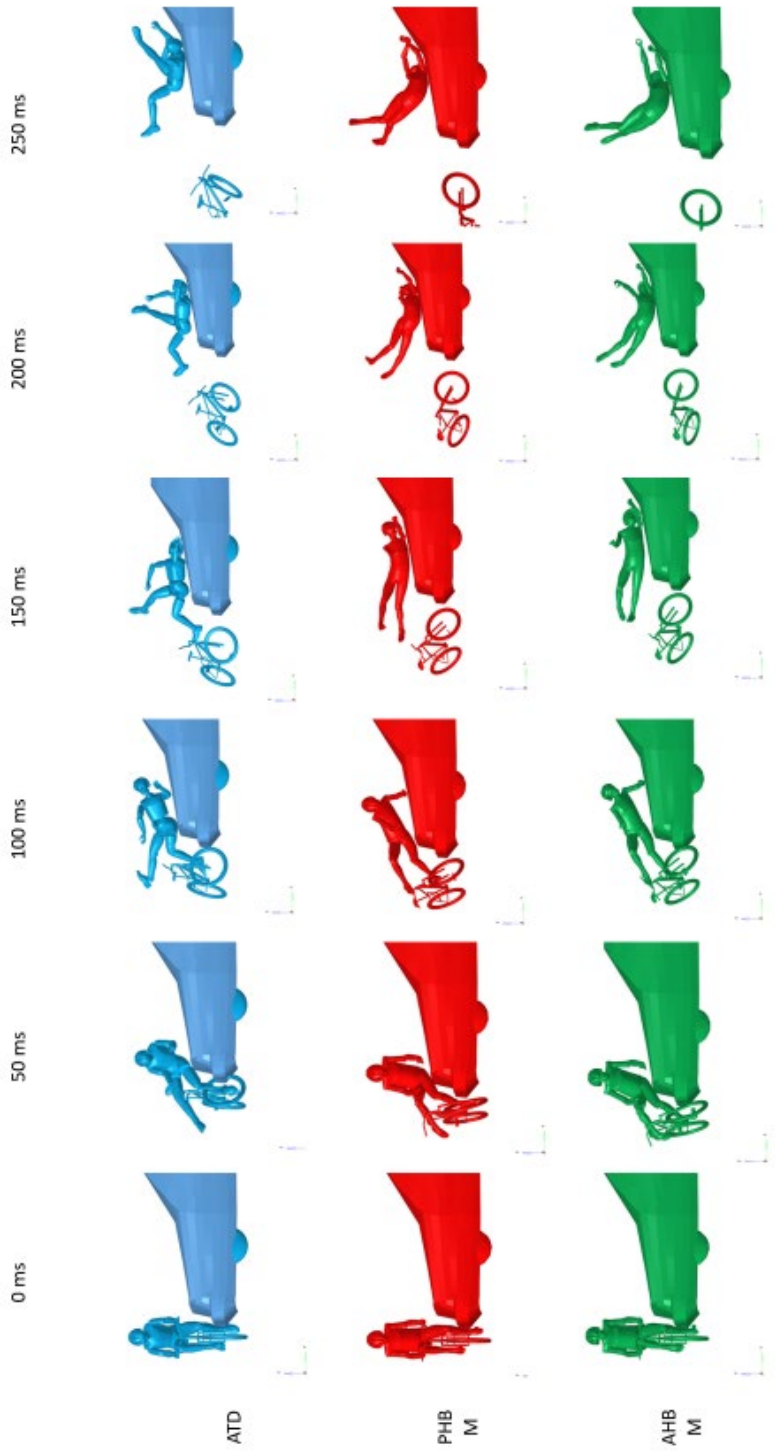

Fig. 18. Impact kinematics in time evolution for the ATD (in blue), PHBM (in red) and AHBM (in green).

Computational resources

The computational cost of the simulations was a non-negligible point to consider for this simulation framework. The usage of Madymo and the human models present in its library provided a faster evaluation of the scenario through the combined MB-FE methodology if compared to equivalent scenarios computed with other FE solvers. An insight of differences in computational resources is shown at Table III. For the ATD and foam scenario, the simulated time was 550 ms. For the AHBM, the simulated time was 850 ms. In the simulations performed in [6] the simulated time was 300 ms.

TABLE IV
CPU USAGE FOR SIMULATIONS AND COMPARISON WITH [18]

Simulation – simulation type	Number of elements	Number of CPUs	Simulation Time	Computational Time
ATD – without foam	101.4 k – whole model	12 CPUs (SMP)	550 ms	47 min
ATD- with foam	106.5 k – whole model	12 CPUs (SMP)	550 ms	1 h 11 min
HBM -without foam	98.4 k – whole model	16 CPUs (SMP)	850 ms	41 min
HBM – with foam	103.5 k – whole model	16 CPUs (SMP)	850 ms	1 h 8 min
Maier – combined MB/FE model	Not defined	16 CPUs (SMP)	300 ms	36 min
Maier – Full FE model	377 k – motorcycle only	16 CPUs (MPP)	300 ms	59 h

IV. DISCUSSION

Many works implemented different HBMs, such as the THUMSv4, SAFER HBM and VIVA+ [8][13][22]. At the best of authors' knowledge, this is the only study that implemented the MADYMO FE HBM model in a cyclist crash. The validity of the model has been proved through validation tests [26]. In previous works the effect of pedalling position on injury criteria were analysed [31-32]. However, for this work the pedalling position is not studied, as the comparison between the different human models was performed under the same boundary conditions. The introduction of the safety device provided, a reduction of force and injury criteria associated with the body region to which the safety device was applied. However, this effect was more visible for the ATD. A possible explanation of the variability of effectiveness might be the position of the foam in the ATD, which was placed very close to the force sensing node. Another point is that the Hybrid III model is not designed for side impact, leading to an unrealistic force to the tibia. Even more than the result itself, it is noteworthy that introducing the safety device in the model took very little time. Thus, whenever the physical and geometrical properties of a safety device are known, its integration into the model is rapid, as is the simulation time required. These considerations were also stated in [18], but it is interesting how the workflow to evaluate motorcycle safety was extended/transferred to a first use in bicycle safety evaluation. No validation of the drop tower test for the protective device with Madymo solver was performed in this study, but the same parameters found in [29] were used. A suggestion for future work is to verify through virtual drop test the goodness of validation also on Madymo software. Another possibility is the solvers coupling, which combines LS-Dyna and Madymo solver to optimize the structural and multi-body solution. The HBM showed notable differences in injury scores compared with the ATD, providing more biofidelic responses. Besides the modelling details and the anthropometric data, the main reasons for this were the different impact kinematics of the two models due to the different mechanical body properties and the positions of sensors. A main difference between the kinematics of the ATD and HBM was the head trajectory. This difference might be related to the different neck stiffness between the ATD and the HBM, which consequently led to different injury index. This difference in neck stiffness is mainly driven by the purpose of the Hybrid III, which was developed for frontal impact crashes, and might not represent in a biofidelic way the response out of his load range and conditions. The introduction of active muscular elements (especially in the neck and spine area) did not change the general kinematic in a drastic way in the leg and thorax area. However, the muscular activation of the neck was needed to not have unrealistic bending of the neck, as can be seen in Fig.17. Nonetheless, the %MVC values were not precise for every muscular group, due to the fact that in the MADYMO solver it is possible to tune only muscle groups, rather than the activation value of every single muscle.

For this reason, it would be interesting to pursue in the future a more detailed study of more precise %MVC values with different AHBMs. The present approach could also be extended to other VRUs, such as electric scooter riders, who face similar collision dynamics with passenger vehicles but exhibit different posture and impact kinematics compared to cyclists. Overall, the study shows that it is worthwhile to analyse the crash of a VRU, such as a cyclist, using HBM and that this approach might be useful for future design choices in passenger cars to improve vehicle safety. Most of the previous work implemented either whole MB models or full FE models [6][32]. The use of a combined MB/FE approach allowed to reduce the computational costs of the simulation, yet being able to provide a detailed analysis of the injury criteria and the kinematics of the impact. The adoption of a deformable MB model, instead of a rigid body car might be beneficial to the overall biofidelity of impact

kinematics [33]. A model with less complex details, led to smaller computational time. This reflects a purpose of the study: how to rapidly explore a design of experiment (DOE) to assess the performance of different passive safety devices.

V. CONCLUSION

This study proposed a combined MB/FE approach for the evaluation of passive safety devices to be implemented in VRU injury scenarios. The study was conducted with both ATD and HBM in a standardised scenario, to establish differences in impact kinematics and how they could change the injury scores compared to passive models. The passive safety device used in this study was an energy-absorber cushion made of PU foam, placed in the region of first impact between the car and the cyclist. The results obtained from the study show that the use of the HBM is noteworthy, not only because of quantitative changes in injury scores, but also because of the significant changes in body trajectories. The HBM can be placed on the bicycle through muscular activation, but some expedients should be taken to permit the HBM to follow the reference position. This does not exclude the possibility that more complex human models might allow pure positioning with only muscular activation. The safety device caused significant changes to the injury scores for the affected body regions (lower leg for this scenario). This approach is scalable to any safety device of interest, paving the way for faster evaluation of innovative design choices prior to the product development stage. Another advantage of this approach is the compromise between the level of modeling details and the computational cost of the simulations.

VI. ACKNOWLEDGEMENTS

The authors would like to thank Prof. A. Schwab for providing data about different bicycles and A. Marekar for support with the tools and the software. We would also like to thank Politecnico di Torino for financial support with outgoing mobility funds dedicated to Master thesis programs abroad.

VII. REFERENCES

[1] Nuyttens, N. (2020) Facts and Figures - Cyclists – 2020. https://road-safety.transport.ec.europa.eu/system/files/2021-07/facts_figures_cyclists_final_20210323.pdf. [2026-02-01].

[2] Schepers, P., Agerholm, N., *et al.*, (2015) An international review of the frequency of single-bicycle crashes (SBCs) and their relation to bicycle modal share. Injury Prevention, **21**: pp. 138-143.

[3] Michal Bíl, Martina Bílová, Ivo Müller, (2010) Critical factors in fatal collisions of adult cyclists with automobiles. Accident Analysis & Prevention, **42**(6): pp. 1632-1636.

[4] Schubert, A., Campolettano, E., Scanlon, J., McMurry, T., Unger, T. (2024) Bridging the gap: Mechanistic-based cyclist injury risk curves using two decades of crash data. Traffic Injury Prevention, **25**(3): pp. S105-S115.

[5] UN, Uniform provisions concerning the approval of motor vehicles with regard to their pedestrian safety. Performance. https://unece.org/fileadmin/DAM/trans/main/wp29/wp29regs/2018/R127r2e.pdf. [2026-02-01].

[6] van Schijndel, M., de Hair, S., Rodarius, C., Fredriksson, R. (2012) Cyclist kinematics in car impacts reconstructed in simulations and full-scale testing with Polar dummy. *Proceedings of the IRCOBI Conference*, 2012, Dublin, Ireland.

[7] DEKRA Automobil Gmbh, Car collides with bicycle. https://www.dekra-roadsafety.com/en/car-collides-with-bycicle/. [2026-05-28]

[8] Brolin, K., Alvarez, V., Säther, A., Olsson, D., Wendelrup, H. (2022) Simulation of bicycle accidents using human body models. *Congress of the European Society of Biomechanics*, 2022, Porto, Portugal.

[9] Niska, A., Wenäll, J., Karlström, J., (2022) Crash tests to evaluate the design of temporary traffic control devices for increased safety of cyclists at road works. Accident Analysis & Prevention, 166 106529.

[10] Niska, A., Wenäll, J. (2019) Simulated single-bicycle crashes in the VTI crash safety laboratory. Traffic Injury Prevention, **20**(3), pp. 68–73.

[11] Raslavicius, L., Bazaras, L., *et al*. (2017) Assessment of bicycle–car accidents under four different types of collision. SAGE publications, **231**(3): pp. 222–234.

[12] Maier, S., Doleac, L., Hertneck, H., Stahlschmidt, S., Fehr, J. (2020) Evaluation of a Novel Passive Safety Concept for Motorcycles with Combined Multi-Body and Finite Element Simulations. *Proceedings of the IRCOBI Conference*, 2020, Munich, Germany.
[13] Klug, C., Feist, F., Wimmer, P. (2018) Simulation of a Selected Real World Car to Bicyclist Accident using a Detailed Human Body Model. *Proceedings of the IRCOBI Conference*, 2018, Athens, Greece.
[14] Sun, J., Li, Z., *et al*. (2018) Identification of pre-impact conditions of a cyclist involved in a vehicle–bicycle accident using an optimized MADYMO reconstruction combined with motion capture. Journal of Forensic and Legal Medicine, **56** : pp. 99-107.
[15] Edwards, A., Forman, L., *et al*. (2025) Model Traceability Procedure for an Automotive-Safety Virtual Testing Framework. *Proceedings of the IRCOBI Conference*, 2025, Vilnius, Lithuania.
[16]Katsuhara, T., Miyazaki, H., Kitagawa, Y., Yasuki, T. (2014) Impact Kinematics of Cyclist and Head Injury Mechanism in Car-to-Bicycle Collision. *Proceedings of the IRCOBI Conference,* 2014, Berlin, Germany.
[17] Pipkorn, B., Alvarez, V., Fahlstedt, M., Lundin, L. (2020) Head Injury Risks and Countermeasures for a Bicyclist Impacted by a Passenger Vehicle. *Proceedings of the IRCOBI Conference,* 2020, Munich, Germany.
[18] Maier, S., Fehr, J. (2024) Efficient simulation strategy to design a safer motorcycle. *Multibody System Dynamics*, **60**: pp. 289–316.
[19] Kleinbach, C., Martynenko, O., *et al*. (2017) Implementation and validation of the extended Hill-type muscle model with robust routing capabilities in LS-DYNA for active human body models. *BioMedical Engineering OnLine*, **16**(109).
[20] Trube, N., Lerge, P., *et al*. (2024) Development and plausibility assessment of an active human body model in numerical cyclist-to-vehicle collision simulations based on real-life accident data. *Proceedings of the IRCOBI Conference*, 2024, Stockholm, Sweden.
[21] Devane, K., Hsu, F., *et al*. (2023) Assessment of finite element human body and ATD models in estimating injury risk in far-side impacts using field-based injury risk. Accident Analysis & Prevention, 192 107274.
[22] Östh, J., Larsson, E., Jakobsson, L. (2022) Human Body Model Muscle Activation Influence on Crash Response. *Proceedings of the IRCOBI Conference,* 2022, Porto, Portugal.
[23]Reichelt, F., Holder, D., Thomas, M. (2023) The Vehicle Development Process Where Engineering Meets Industrial Design. IEEE Engineering Management Review, **51**(4): pp. 102–123.
[24] Maier, S., Doleac, L., Hertneck, H., Stahlschmidt, S., Fehr, J. (2021) Finite Element Simulations of Motorcyclist Interaction with a Novel Passive Safety Concept for Motorcycles. *Proceedings of the IRCOBI Conference*, 2021, Online.
[25] Kalsbeek, I. (2016) Experimental investigation into the shimmy motion of the bicycle for improving model-based shimmy estimations. https://repository.tudelft.nl/record/uuid:a98d51c1-7754-4c29-b883-f130ba05136b. [2025-11-25].
[26] Siemens IndustrySoftware and Services BV (2020) Simcenter Madymo Model Manual.
[27]Ricard, M., Hills-Meyer, P., Miller, M., Michael, T. (2006) The effects of bicycle frame geometry on muscle activation and power during a wingate anaerobic test. *Journal of Sports Science and Medicine*, **5**(1): pp. 25–32.
[28] Pratellesi, A., Turrin, S., Haag, T., Scippa, A., Baldanzini, N. (2011) On the effect of testing uncertainties in the homologation tests of motorcycle helmets according to ECE 22.05. International Journal of Crashworthiness, **16**(5): pp. 523-536.
[29]Maier, S., Helbig, M., Hertneck, H., Fehr, J. (2021) Maier, 2021, Characterisation of an Energy Absorbing Foam for Motorcycle Rider Protection in LS-DYNA. 13th European LS-Dyna Conference, 2021, Ulm, Germany.
[30] Kleinberger, M., Sun, E., Eppinger, R. (1998) Injury Criteria for the Assessment of Advanced Automotive Restraint Systems. https://www.nhtsa.gov/sites/nhtsa.gov/files/criteria.pdf. [2026-01-20].
[31] Oikonomou, M., Iraeus, J., *et al*. (2024) Characterising Bicyclist Posture in Various Bicycle Types for Safety Evaluation. *Proceedings of the IRCOBI Conference, 2024,* Stockholm, Sweden.
[32] Ito, D., Yamada, H., Oida, K., Mizuno, K. (2014) *Finite element analysis of kinematic behavior of cyclist and performance of cyclist helmet for human head injury in vehicle-to-cyclist collision,* Berlin, Germany.
[33] Ambrósio, J. (2005) Crash analysis and dynamical behaviour of light road and rail vehicles. Vehicle System Dynamics, **43(**6–7): pp. 385-411.